Lithos 228–229 (2015) 43–54

Contents lists available at ScienceDirect

Lithos

journal homepage: www.elsevier.com/locate/lithos

Ancient oceanic crust in island arc lower crust: Evidence from oxygen isotopes in zircons from the Tanzawa Tonalitic Pluton

Kazue Suzuki [a,*], Kouki Kitajima [b], Yusuke Sawaki [a], Kentaro Hattori [c], Takafumi Hirata [c], Shigenori Maruyama [d]

[a] Department of Earth and Planetary Sciences, Tokyo Institute of Technology, 2-12-1, O-okayama, Meguro-ku, Tokyo, Japan
[b] WiscSIMS, Department of Geoscience, University of Wisconsin, 1215, W. Dayton St., Madison, WI 53706, USA
[c] Division of Earth and Planetary Sciences, Kyoto University, Kitashirakawa, Oiwake-cho, Sakyo-ku, Kyoto, Japan
[d] Earth-Life Science Institute, Tokyo Institute of Technology, 2-12-1, O-okayama, Meguro-ku, Tokyo, Japan

ARTICLE INFO

Article history:
Received 11 November 2014
Accepted 15 April 2015
Available online 25 April 2015

Keywords:
Arc lower-crust
Oceanic crust
Zircon oxygen isotope
Tanzawa Tonalitic Pluton
IBM arc

ABSTRACT

Knowledge of the lithological variability and genesis of island arc crust is important for understanding continental growth. Although the volcanic architecture of island arcs is comparatively well known, the nature of island arc middle- and lower-crust remains uncertain owing to limited exposure. One of the best targets for deciphering the evolution of an island arc system is the Tanzawa Tonalites (4–9 Ma), in the intra-oceanic Izu–Bonin–Mariana arc. These tonalities which occupied a mid-crustal position were generated by partial melting of lower crust. To constrain protoliths of the plutonic rocks in the island arc lower crust, *in-situ* O-isotopic analysis using an IMS-1280 Secondary Ion Mass Spectrometer was carried out on 202 zircon grains separated from 4 plutons in the Tanzawa Tonalite. $\delta^{18}O$ value of the zircons ranges from 4.1‰ to 5.5‰ and some zircons have $\delta^{18}O$ slightly lower than the mantle range. The low zircon $\delta^{18}O$ values from the Tanzawa Tonalite suggest that their protoliths involved materials with lower $\delta^{18}O$ values than those of the mantle. Hydrothermally altered gabbros in the lower oceanic crust often have lower $\delta^{18}O$ values than mantle and can be primary components of arc lower crust. The Tanzawa Tonalite is interpreted to have been formed by partial melting of island arc lower crust. Thus the low $\delta^{18}O$ values in zircons from the Tanzawa Tonalites may originate by melting of the hydrothermally altered gabbro. Ancient oceanic crustal material was likely present in the Izu–Bonin–Mariana arc lower crust, at the time of formation of the Tanzawa Tonalites.

1. Introduction

Arc magmatism in subduction zones is recognized as a predominant mechanism for continental growth, because trace element patterns in arc crust are similar to those of continental crust (e.g., Rudnick, 1995). The average chemical composition of continental crust is andesitic (e.g., Taylor and White, 1965), and andesite is an important product of arc magmatism. Therefore, constraining the chemical composition and formation of immature arc crust can lead to a better understanding of the initial stage of the continental crustal growth. The Izu–Bonin–Mariana arc (IBM arc; Fig. 1A) in the Western Pacific Ocean is an active and immature intra-oceanic arc, and has attracted much interest from seismological and geochemical studies to reveal its structure and composition (e.g., Suyehiro et al., 1996; Cosca et al., 1998; Ishizuka et al., 2006; Takahashi et al., 2007; Reagan et al., 2010). Seismic investigations combined with geochemical data for exposed rocks suggest the presence of a ~5 km thick tonalitic middle crust overlying mafic lower crust in northern Izu arc, Mariana arc and West Mariana ridge (Suyehiro et al., 1996; Kitamura et al., 2003; Takahashi et al., 2007). Based on the seismic structure of the arc, evolution models from oceanic crust to present IBM arc were proposed by some researchers (e.g., Tatsumi et al., 2008). In general, the previous studies have focused on the process for generation and addition of new arc crust (e.g., Kuno, 1968; Garrido et al., 2006; Tatsumi et al., 2008), but not on the pre-existing oceanic crust in an immature arc. Kuno (1968) implied that ancient oceanic crust may be incorporated into island arc crust during the early stages of its evolution. For example, a *ca.* 10 km thick layer of oceanic crust has been imaged seismically in the mid crust below the Aleutian arc along the northwestern margin of Pacific Ocean (Holbrook et al., 1999; Shillington et al., 2004). Unfortunately geochemical evidence alone is insufficient to confirm the existence of former oceanic crust in island arcs because of difficulty of sampling. Nevertheless Kay et al. (1986) reported radiogenic Nd isotopic compositions from xenoliths and volcanic rocks that they interpreted as evidence for the presence of oceanic crust in the island arc crust. However, the Aleutian arc may not be a good analogue of other island arcs because the seismic structure of the Aleutian arc is clearly different from that of the IBM arc. For example the IBM arc has a ~5 km thick felsic middle layer, that is absent from the Aleutian arc (Suyehiro et al., 1996; Takahashi et al., 2007).

A number of studies have shown that deep parts of the continental crust can be exposed in collision zones (e.g., Fountain and Salisbury,

* Corresponding author. Tel.: +81 3 5734 2618; fax: +81 3 5734 3538.
E-mail addresses: suzuki.k.ae@m.titech.ac.jp, suzuki.k@eps.s.u-tokyo.ac.jp (K. Suzuki).

http://dx.doi.org/10.1016/j.lithos.2015.04.005
0024-4937/

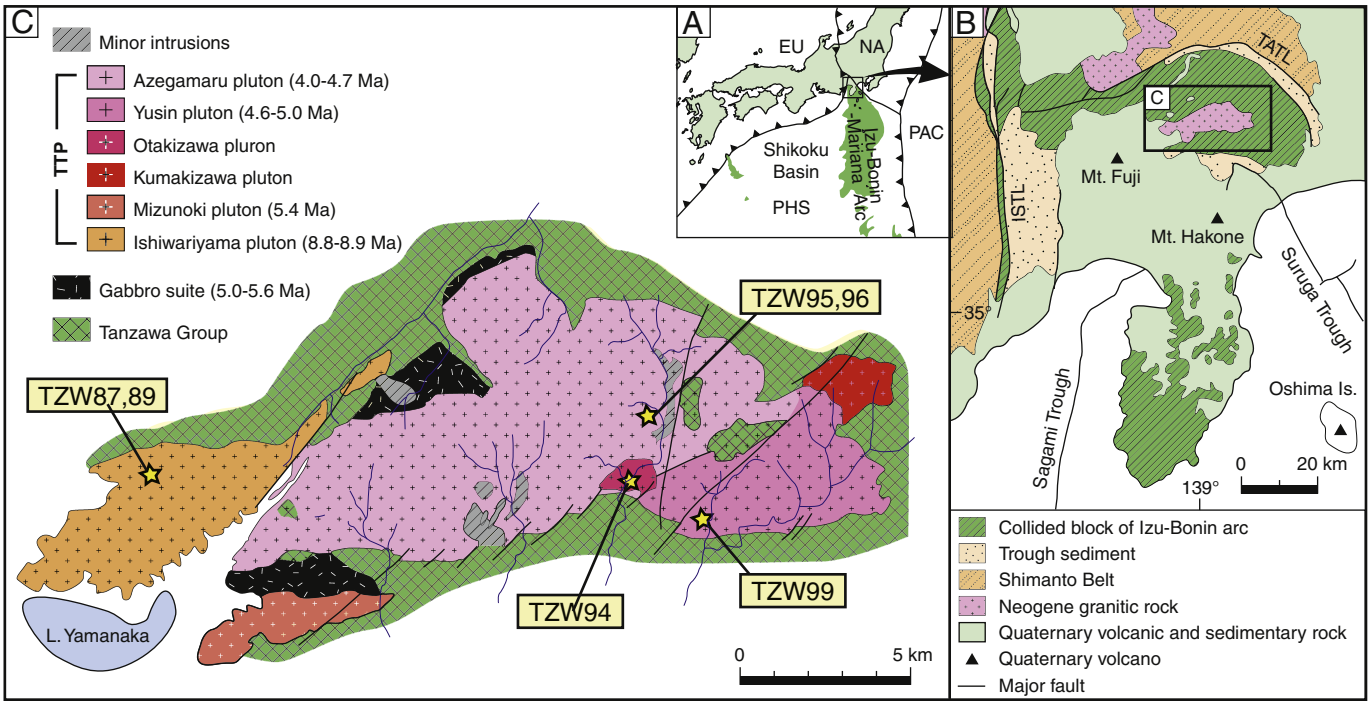

Fig. 1. (A) Tectonic map of the northern end of the IBM-arc. EU, Eurasian Plate; NA, North American Plate; PHS, Philippine Sea Plate; PAC, Pacific Plate. (B) Geological map of the Izu-Collision-Zone. ISTL, Itoigawa–Shizuoka tectonic line; TATL, Tonoki-Aikawa tectonic line. (C) Geological map of the Tanzawa Tonalitic Pluton (modified from Kawate and Arima (1998)) showing sampling localities. We collected tonalities from Ishiwariyama, Otakizawa, Yusin and Asegamaru plutons. Age data are from Tani et al. (2010).

1981; Mezger, 1992). A similar situation occurs in the Tanzawa Block in the Izu-Collision-Zone with the exposure of tonalitic rocks younger than 9 Ma (e.g. Tani et al., 2010) due to collision between the active IBM arc and the Honshu arc. The Tanzawa Tonalite is interpreted to be the mid crust of the proto-IBM arc. It exhibits the geochemical characteristics and isotopic features of M-type granites, i.e., low K content and unradiogenic initial Sr isotopic composition (Ishihara et al., 1976; Kawate and Fujimaki, 1996). It is also similar to felsic igneous rocks in the IBM (Ishizaka and Yanagi, 1977; Takahashi, 1989; Kawate and Arima, 1998). Thus, the Tanzawa Tonalite is an excellent suite to trace process during island arc evolution, from oceanic crust to mature arc crust. The experimental research (Nakajima and Arima, 1998) suggests that the Tanzawa Tonalites were generated by partial melting of mafic lower crust of the IBM arc. This implies that the Tanzawa Tonalite inherited the chemical characteristics of deeper part of the proto-arc crust. However, although U–Pb ages and REE data for zircon in mafic enclaves in the Tanzawa Tonalite were derived from the arc lower crust (Suzuki et al., 2014), the protoliths containing these zircons have not yet been identified.

Oxygen isotope data for whole rocks and minerals have been used to constrain the nature of protolith that were melted to form volcanic and plutonic rocks (e.g., Matsuhisa, 1979; Lackey et al., 2008). Although Ishihara and Matsuhisa (2005) determined whole rock oxygen isotope ratios for samples of Tanzawa Tonalite, they could not constrain $\delta^{18}O$ of the source rocks, because whole rock oxygen isotope ratios increase with increasing SiO_2 content (Matsuhisa, 1979; Taylor and Sheppard, 1986; Lackey et al., 2008) and because magmatic whole rock $\delta^{18}O$ is commonly overprinted by subsolidus alteration. However, oxygen isotopic ratios of non-metamict zircons are resistant to alteration and effectively reflect the $\delta^{18}O$ of their parental host rock through the whole rock-zircon fractionation factor (Valley et al., 1994; Lackey et al., 2008).

Therefore, to better understand the nature of the lower arc crust and thus, the evolution of intra-oceanic arcs, we performed *in-situ* O-isotopic analysis on zircon grains separated from the 4 tonalitic plutons (Ishiwariyama, Otakizawa, Yusin, Azegamaru) in the Tanzawa Block. The data was obtained using a secondary ion mass spectrometer (SIMS), combined with *in-situ* trace element analysis using laser ablation-inductively coupled plasma-mass spectrometer (LA-ICP-MS).

2. Geology

2.1. Geological setting of the Tanzawa Tonalitic Pluton

The IBM arc has been formed by subduction of Pacific Sea plate beneath the Philippine Sea plate, and has collided with the Honshu arc in the Izu-Collision-Zone, central Japan (Fig. 1A; Matsuda, 1978). The Tanzawa block is located in the Izu-Collison Zone, *ca.* 300 km northwest of the triple junction of the Eurasia, North America, and Philippine Sea plates (Fig. 1B). The Tanzawa block has three main components: (1) the Tanzawa Group (3–17 Ma), (2) the Tanzawa gabbro suite (5–6 Ma), and (3) the Tanzawa Tonalitic Pluton (TTP; 4–9 Ma). The Tanzawa Group, with thickness estimated to be greater than 10 km (Takita, 1974), is composed mainly of basaltic volcaniclastic rocks deposited at *ca.* 3–17 Ma. The group was initially formed in a pelagic environment before 11 Ma (Shimazu, 1989; Aoike et al., 1995) as part of the upper crust of the IBM arc, and approached near the Honshu arc via continuous movement of the Philippine Sea Plate to the north. The age of the gabbro suite is constrained from zircon U–Pb dating using SHRIMP-II (5–6 Ma; Tani et al., 2010). The relationship between the Tanzawa Group and gabbro suite is not clear because of limited exposure, but in areas, the Group is intruded by the gabbro suite (Aoike et al., 1997). Both of them are cut by the TTP (Takita, 1974).

The TTP includes tonalite and quartz-diorite, both of which are rich in magnetite with high magnetic susceptibility (Ishihara et al., 1976). Based on its very low K_2O (mainly 0.13 to 1.90 wt.%; Ishihara et al., 1976; Kawate and Arima, 1998; Takahashi et al., 2004), low K_2O/Na_2O (<0.55; Ishihara et al., 1976; Kawate and Arima, 1998), low Rb, Rb/Sr and moderately high K/Rb (541–630; Ishizaka and Yanagi, 1977), and extremely unradiogenic initial $^{87}Sr/^{86}Sr$ ratios near the mantle value (0.70331–0.70370; Kawate and Fujimaki, 1996), the Tanzawa Tonalite is interpreted to have the most typical characteristics of M-type granite compared to the other granitoids in Japan (Takahashi, 1985).

Geochemical characteristics and P-wave velocities of the TTP rocks are similar to felsic igneous rocks in the IBM arc (Ishizaka and Yanagi, 1977; Takahashi, 1989; Suyehiro et al., 1996; Kawate and Arima, 1998; Kitamura et al., 2003). Therefore, the TTP is interpreted to be the exposed middle crust (at depths ranging from 5 km to 10 km) of the IBM arc, and to have been formed in an immature arc environment.

After the initial recognition of the TTP (Takita, 1974; Sugiyama, 1976), Kawate and Arima (1998) subdivided the TTP and gabbro suites. Although the ages of the TTP were originally obtained by K–Ar and Ar–Ar analyses (4.3–10.7 Ma: Kawano and Ueda, 1966; Sato et al., 1986; Saito, 1993), Saito (1993) showed that there was a problem with the chronology due to the problem of excess Ar. Based on field relationships, U–Pb zircon geochronology and fission-track analysis, the TTP is now subdivided into 8 plutonic intrusive events and 5 stages (Fig. 1C; Yamamoto and Kawakami, 2005; Yamada and Tagami, 2008; Tani et al., 2010; Suzuki et al., 2014). These are: Stage 1 — Ishiwariyama pluton (8–9 Ma), Stage 2 — Gabbro suite (5–6 Ma), Stage 3 — Kumakitazawa, Mizunoki and Otakizawa plutons (not dated), Stage 4 — Azegamaru and Yusin plutons (4—5 Ma) and Stage 5 — minor intrusions. The U–Pb zircon ages from the Mizunoki, Azegamaru and Yusin pluton (4.0–5.4 Ma; Tani et al., 2010; Suzuki et al., 2014) are contemporaneous with the collision of the Tanzawa block with the Honshu Arc (3.8–6.8 Ma; Yamamoto and Kawakami, 2005). This suggests that magmatism of Tanzawa tonalities, except for Ishiwariyama pluton, was syn-collisional. Tani et al. (2010) also suggested the involvement of terrigenous clastics from the Honshu arc to the magma source, based on elevated Th/Nb ratios in zircons from the Tanzawa Tonalites.

Genesis of the granitoids in the IBM arc by slab-melting is not possible because of the age of the subducted slab (>130 Ma; Müller et al., 1997). Models for the formation of the TTP therefore favored crystal fractionation and accumulation processes from an intermediate parental magma (Kawate and Arima, 1998; Takahashi et al., 2004), generated by dehydration partial melting of amphibolites in the lower crust of IBM arc (Nakajima and Arima, 1998). The existence of ~10 km thick mafic lower crust in the IBM arc was confirmed from seismic observations (Suyehiro et al., 1996; Kitamura et al., 2003). Age of the arc lower crust beneath the TTP is estimated from U–Pb age of zircons in mafic enclaves included in the TTP (Suzuki et al., 2014). The zircon ages ranging from 4 to 43 Ma and age of surrounding geological components of the TTP, which are gabbro suites (5–6 Ma; Tani et al., 2010), the Tanzawa Block (3–17 Ma; Aoike, 1999) and arc lower crust, suggest that zircons older than 17 Ma probably come from arc lower crust beneath the TTP. Distinct characteristics of these older zircons such as lower Eu/Eu* ratio and irregular shape compared to zircons in the Tanzawa Tonalite support the explanation (Suzuki et al., 2014). Based on the oldest age of zircon from the mafic enclaves, the arc lower crust beneath the Taznawa Tonalite is suggested to be formed >43 Ma.

Based on the time interval of formation age between the Ishiwariyama pluton (Stage 1) and the main body of the TTP (Stages 3 and 4), it is suggested that the partial melting events (and following crystal fractionation) occurred before and during the arc collision. In this study, we collected tonalite samples from Ishiwariyama, Otakizawa, Azegamaru and Yusin types (Fig. 1C) to cover each stage of tonalite generation.

2.2. Petrography of tonalite

Photographs of a rock specimen and thin sections of the tonalite from the Azegamaru pluton (TZW96) are shown in Fig. 2. We collected fresh outcrop samples from the Otakizawa, Azegamaru and Yusin plutons (Fig. 2-a). Because the tonalites at the Ishiwariyama are generally strongly altered, we used both an outcrop sample (TZW87) and a fresh boulder sample (TZW89). As some tonalites contain mafic enclaves, these were avoided during analyses. The tonalites are composed of medium- to coarse-grained silicate minerals and display equigranular

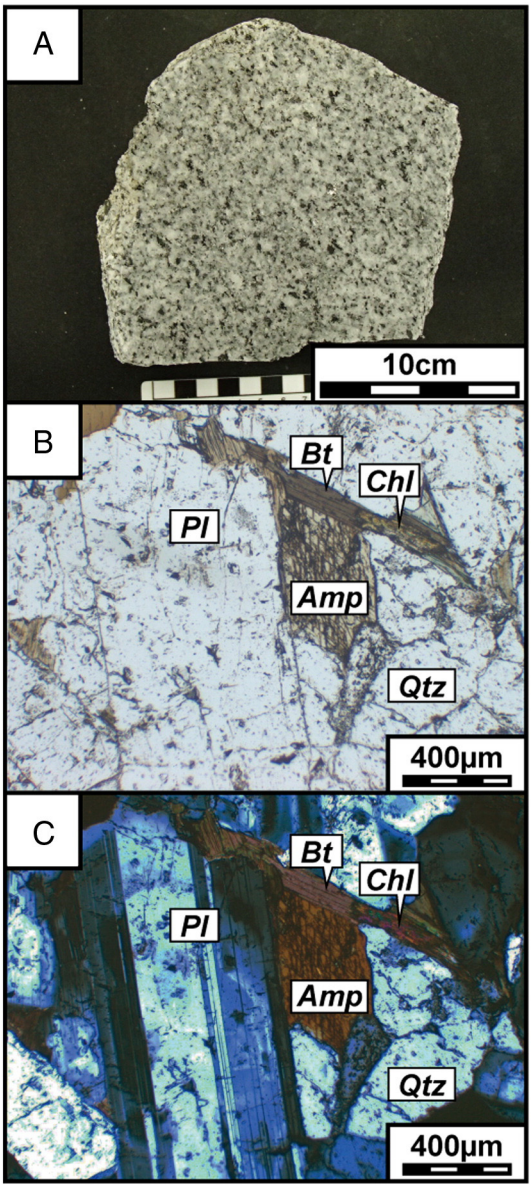

Fig. 2. (A) Photographs of a tonalite sample collected from Azegamaru pluton (TZW96). (B, C) Micro-photographs taken in plane and cross-polarized light for a representative tonalite (TZW96).

textures. The rocks mainly consist of plagioclase, quartz, hornblende, biotite with minor amounts of K-feldspar (Figs. 2B and C). The grain sizes are variable, and their average length is *ca.* 1 mm. Chlorite, actinolite and epidote are secondary minerals. Accessory minerals are magnetite, ilmenite, zircon, apatite, and sphene. All samples are plotted in the tonalite field in the Q–A–P modal diagram from Streckeisen (1976).

3. Sample preparation and analytical procedures

3.1. Whole rock compositions

Six tonalite samples were prepared for whole rock chemistry. Thin (1–2 cm thick) rock chips weighing about 20 g were cut from fresh parts of the samples. Visible mafic enclave parts in tonalite were avoided during this process. The chips were washed with distilled water using an ultrasonic device, dried completely at 120 °C, and then crushed using a tungsten-carbide mill and an agate-ball mill. $H_2O(-)$ and loss on ignition (LOI) of rock powders were determined at 110 °C and 950 °C (over 6 h), respectively.

Major element compositions (Si, Ti, Al, Fe, Mn, Mg, Ca, Na, K and P) were analyzed using fused glass disks by X-ray fluorescence spectrometer (XRF; RIX 2100, RIGAKU) at the Tokyo Institute of Technology, Japan. Glass disks were prepared with lithium tetraborate flux ($Li_2B_4O_7$) in a dilution ratio of 1:10 at 1050 °C. The accelerating voltage was 50 kV and current was 50 mA during the XRF analysis. Calibration methods using GSJ standards are after Machida et al. (2008). The repeated analyses of same standard indicate reproducibility of this analysis was better than 1%, except for Na and P (<5%).

3.2. Zircon separation and in-situ oxygen isotope analysis

Zircon grains were separated from 2 tonalites samples from the Ishiwariyama and the Azegamaru plutons, and 1 tonalite sample from the Otakizawa and the Yusin plutons, using standard crushing, panning and magnetic-separation techniques. The grains were mounted in 25 mm epoxy disks with chips of KIM-5 standard zircon (Valley et al., 1998; Valley, 2003) and polished until the midsections of the grains were exposed. The internal structures of the zircons and the presence of inclusions were checked using transmitted and reflected light optical microscopy and cathodoluminescence (CL) imaging. The CL images were acquired using a Hitachi S-3400 N scanning electron microscope (Hitachi High Tech. Corp., Japan) with a Chroma CL2 sensor (Gatan, Inc., USA) at the Tokyo Institute of Technology.

Before oxygen isotope analysis, the epoxy mount was washed with de-ionized water and ethanol using an ultrasonic bath. Mounts were dried in Nitrogen gas prior to coating with gold for SIMS oxygen isotope analysis. Oxygen isotope ratios in zircons were determined using CAMECA IMS-1280 in the WiscSIMS Laboratory at the University of Wisconsin-Madison. Analytical procedures are followed to those reported by Kita et al. (2009). *In-situ* oxygen isotopes were analyzed using a 2.0–2.2 nA primary Cs^+ beam with ~10 μm spot size. Secondary ^{16}O and ^{18}O ions were measured simultaneously using two Faraday cup detectors. KIM-5 zircon ($\delta^{18}O = 5.09‰$ relative to Vienna Standard Mean Ocean Water (VSMOW); Valley, 2003) was used as a standard, and the average value of eight standard analyses bracketing each 10 analyses of unknowns was used to correct instrumental bias. The precision of each analysis is estimated by two standard deviations (2SD) of the reproducibility of bracketing standard analyses and is *ca.* 0.3‰ on average. The oxygen isotope ratios are reported in standard per mil notation relative to VSMOW (Table 1).

3.3. In-situ U–Pb age and trace-element analyses

Trace element concentrations and U–Pb ratios in zircons were determined by laser ablation-inductively coupled plasma-mass spectrometry (LA-ICP-MS) after oxygen isotope analysis. The ICP-MS (Thermo Scientific iCAP-Q, Kyoto University) is equipped with a ESI New Wave Research ArF Excimer laser ablation system (NWR193) operating at 193 nm wavelength. As a carrier gas, He was mixed with Ar to improve the sample transport efficiency from the sample cell to the MS, as well as to reduce the sample deposition around the ablation pit (Eggins et al., 1998). In this study, charcoal filter was adopted onto the Ar carrier gas in order to reduce the mass spectrometric interferences on ^{204}Pb by ^{204}Hg (Hirata et al., 2005). Residual contribution of ^{204}Hg was corrected by subtracting the signal intensity of ^{204}Hg estimated by the signal intensity of ^{202}Hg. Signal smoothing device was adopted between the sample cell and the torch, which improve the stability of the signal intensity (Tunheng and Hirata, 2004).

Operational settings such as Ar–He gas flow rate, lens biases and mass resolution were optimized to maximize the intensity of the ^{29}Si signal obtained by laser ablation of NIST SRM610 with the $^{232}Th^{16}O^+/^{232}Th^+$ ratio <1%. All measurements were carried out by peak-jumping. The 91500 zircon (Wiedenbeck et al., 2004) and OD-3 were used as primary and secondary standards to correct the effects of U–Pb fractionation and mass discrimination of the mass spectrometer. NIST 610 and 612 glasses (Pearce et al., 1997) were used as standards for estimation of the trace element concentration. Further analytical procedures are shown in Table S1 in the Supplementary information. We monitored ^{204}Pb during ICP-MS analysis, and excluded the U–Pb ages of zircons with clearly higher ^{204}Pb abundances than the gas blank from data presented in tables.

4. Results

4.1. Whole-rock compositions

Whole-rock chemical compositions of the Tanzawa Tonalite are listed in Table S2 in the Supplementary information. The tonalites from 4 plutons range in SiO_2 and MgO between 64.9 and 71.0 wt.% and 1.11 to 1.96 wt.%, respectively. Compared to previous studies of the Tanzawa Tonalite (Kawate and Arima, 1998; Takahashi et al., 2004), these are relatively felsic compositions. Their low K contents (0.76 to 1.68 wt.%) and low K_2O/Na_2O ratio (0.20 to 0.48) are consistent with the petrologic description (K-feldspar-poor mineral assemblage) and character of M-type granites.

4.2. Zircon morphology and CL images

Representative CL images of zircons are shown in Fig. 3. Zircons in the Tanzawa Tonalite typically display euhedral shapes with dimensions generally ranging from 50 × 50 to 100 × 200 μm and are colorless. Typical zircons from the Ishiwariyama pluton (TZW87, 89) are smaller than those from the other plutons (Figs. 3A and B). Zircons from the Otakizawa pluton (TZW94) typically display elongated shapes with the dimensions of 30 × 150 μm (Fig. 3C).

All of these zircons display blue color, and some parts are pale green in the CL observation (Fig. 3). The zircons generally display clear oscillatory zoning and/or sector zoning from core to rim, whereas some of zircons from the Ishiwariyama and Azegamaru plutons (TZW89, TZW95, and TZW96) display bright homogeneous rim sharply distinguished from zoning region. These rims are typically shown in zircons from the TZW95 (Fig. 3E), but there is no significant difference in mineral assemblage among these rocks. Many zircons in the Otakizawa pluton display banded texture in the CL images (Fig. 3C). These characteristics of zircons from Otakizawa pluton (banded texture and elongated shape) are similar to those of zircons crystallized in relatively undifferentiated magma such as diorites (Corfu et al., 2003).

4.3. Oxygen isotope composition in zircon

The oxygen isotope compositions in zircons are shown in Table 1 and Fig. 4. The $\delta^{18}O$ values in zircons from the Ishiwariyama (TZW87, 89), Otakizawa (TZW94) and Yusin (TZW99) plutons range from 4.1‰ to 5.1‰, and display peaks at 4.5–4.9‰ (Fig. 4). The range of the $\delta^{18}O$ values is slightly lower than mantle range constrained from $\delta^{18}O$ of zircons in kimberlite ($\delta^{18}O = 5.3 \pm 0.6‰$ (2SD); Valley et al., 1998) and the range of $\delta^{18}O$ in zircons from modern mid-ocean ridge crust ($\delta^{18}O = 5.2 \pm 0.5‰$ (2SD); Grimes et al., 2011). Additionally, the $\delta^{18}O$ values are similar to those from plagiogranites in Oman ophiolites ($\delta^{18}O = 4.7 \pm 0.7‰$ (2SD); Grimes et al., 2013; Fig. 4). The zircons from these plutons show no significant internal variation of $\delta^{18}O$ within single zircon grain (Fig. 3). The range of $\delta^{18}O$ value in each pluton is nearly similar to the analytical error (±0.3‰), however, zircons from the Azegamaru pluton (TZW95, 96) display wide range of oxygen isotope values. Bright rims in zircon from TZW95 yield low $\delta^{18}O$ values ranging from 3.5‰ to 4.1‰ (average = 3.8 ± 0.4‰), whereas oxygen isotope

Table 1
Oxygen isotope ratios of zircons in the Tanzawa Tonalites.

Analysis no.	$\delta^{18}O$ (Zrc)	2 S.D.	Analysis no.	$\delta^{18}O$ (Zrc)	2 S.D.	Analysis no.	$\delta^{18}O$ (Zrc)	2 S.D.	Analysis no.	$\delta^{18}O$ (Zrc)	2 S.D.	Analysis no.	$\delta^{18}O$ (Zrc)	2 S.D.	Texture	Analysis no.	$\delta^{18}O$ (Zrc)	2 S.D.	Texture
Ishiwariyama pluton						Otakizawa pluton			Yusin pluton			Azegamaru pluton							
TZW 87			*TZW 89*			*TZW 94*			*TZW 99*			*TZW 95*				*TZW 96*			
TZW87-1a	4.59	0.14	TZW89-1	4.93	0.17	TZW94-1a	4.30	0.30	TZW99-1a-1	4.70	0.13	TZW95-1a	5.04	0.25		TZW96-1a	5.19	0.24	
TZW87-2a	4.66	0.14	TZW89-2	4.99	0.17	TZW94-2a	5.04	0.30	TZW99-1b-1	4.66	0.13	TZW95-1b	5.19	0.25		TZW96-2	5.13	0.24	
TZW87-3	4.86	0.14	TZW89-3a	4.48	0.17	TZW94-3a	4.54	0.30	TZW99-3	4.78	0.13	TZW95-3a	5.15	0.25		TZW96-3a	5.28	0.24	
TZW87-4a	4.87	0.14	TZW89-3b	4.77	0.17	TZW94-4a	4.47	0.30	TZW99-4-1	4.51	0.13	TZW95-4a	4.76	0.25		TZW96-4a	4.94	0.24	
TZW87-5a	4.87	0.14	TZW89-5a	4.70	0.17	TZW94-5a	4.68	0.30	TZW99-5-1	4.94	0.13	TZW95-5a	4.96	0.25		TZW96-5	5.22	0.24	
TZW87-6	4.79	0.14	TZW89-5b	4.76	0.17	TZW94-6a	4.70	0.30	TZW99-6	4.80	0.13	TZW95-6a	5.11	0.25		TZW96-6	5.21	0.24	
TZW87-7a	4.96	0.14	TZW89-7	4.89	0.17	TZW94-7a	4.76	0.30	TZW99-7a	4.70	0.13	TZW95-7a	5.03	0.25		TZW96-7	5.38	0.24	
TZW87-8a	4.69	0.14	TZW89-8a	4.89	0.17	TZW94-8a	4.67	0.30	TZW99-8a	4.84	0.13	TZW95-8	4.80	0.25		TZW96-8a	5.30	0.24	
TZW87-9a	4.84	0.14	TZW89-8b	4.69	0.17	TZW94-9a	4.87	0.30	TZW99-9-1	4.65	0.13	TZW95-9a	4.88	0.25		TZW96-9a	5.12	0.24	
TZW87-10a	4.77	0.14	TZW89-10	4.87	0.17	TZW94-10a	4.79	0.30	TZW99-10a	4.88	0.13	TZW95-10a	5.04	0.25		TZW96-10a	5.20	0.24	
TZW87-11a	4.64	0.24	TZW89-11a	4.71	0.09	TZW94-10b	4.54	0.36	TZW99-11a	4.90	0.31	TZW95-11	4.91	0.14		TZW96-11	5.10	0.32	
TZW87-11b	4.67	0.24	TZW89-12a	4.85	0.09	TZW94-12	4.62	0.36	TZW99-12a	4.95	0.31	TZW95-12a	5.33	0.14		TZW96-12	5.15	0.32	
TZW87-13	4.57	0.24	TZW89-12b	4.45	0.09	TZW94-13	4.62	0.36	TZW99-13a	4.81	0.31	TZW95-13a	5.02	0.14		TZW96-13	5.10	0.32	
TZW87-14a	4.64	0.24	TZW89-14	4.83	0.09	TZW94-14	4.69	0.36	TZW99-14	4.95	0.31	TZW95-14	4.97	0.14		TZW96-14a	5.03	0.32	
TZW87-15	4.66	0.24	TZW89-15	4.62	0.09	TZW94-15	4.59	0.36	TZW99-15a	4.89	0.31	TZW95-15a	5.15	0.14		TZW96-15a	5.05	0.32	
TZW87-16a	4.83	0.24	TZW89-16a	4.60	0.09	TZW94-16	4.54	0.36	TZW99-16	4.98	0.31	TZW95-15b	3.82	0.14	Bright rim	TZW96-16a	5.11	0.32	
TZW87-17	4.94	0.24	TZW89-16b	4.86	0.09	TZW94-17a	4.28	0.36	TZW99-17	4.95	0.31	TZW95-17a	5.04	0.14		TZW96-17a	5.19	0.32	
TZW87-18a	4.70	0.24	TZW89-18a	4.67	0.09	TZW94-17b	4.41	0.36	TZW99-18	5.03	0.31	TZW95-17b	3.62	0.14	Bright rim	TZW96-18	5.52	0.32	
TZW87-19	4.79	0.24	TZW89-18b	4.90	0.09	TZW94-17c	4.52	0.36	TZW99-19	4.93	0.31	TZW95-19a	4.68	0.14		TZW96-19a	5.25	0.32	
TZW87-20	4.66	0.24	TZW89-20a	4.94	0.09	TZW94-20a	4.29	0.36	TZW99-20	5.10	0.31	TZW95-29b	3.54	0.14	Bright rim	TZW96-20	5.28	0.32	
TZW87-21	4.80	0.22	TZW89-21	4.64	0.21	TZW94-21a	4.58	0.20	TZW99-8b	4.51	0.22	TZW95-21a	5.06	0.22		TZW96-21a	5.43	0.22	
TZW87-22a	4.91	0.22	TZW89-22	4.50	0.21	TZW94-22a	4.78	0.20	TZW99-10b	4.56	0.22	TZW95-21b	3.93	0.22	Bright rim	TZW96-21b	5.01	0.22	Bright rim
TZW87-23a	4.70	0.22	TZW89-23a	4.62	0.21	TZW94-22b	4.54	0.20	TZW99-15b	4.68	0.22	TZW95-23a	5.03	0.22		TZW96-23a	5.16	0.22	
TZW87-24a	4.93	0.22	TZW89-24a	4.74	0.21	TZW94-24a	4.26	0.20	TZW99-24a	4.76	0.22	TZW95-23b	3.59	0.22	Bright rim	TZW96-23b	4.89	0.22	Bright rim
TZW87-25a	4.54	0.22	TZW89-25a	4.75	0.21	TZW94-25a	4.51	0.20	TZW99-25a	4.87	0.22	TZW95-25a	5.02	0.22		TZW96-25a	5.17	0.22	
TZW87-26	4.82	0.22	TZW89-25b	4.92	0.21	TZW94-26	4.71	0.20	TZW99-26a	4.67	0.22	TZW95-25b	4.85	0.22	Bright rim	TZW96-25b	4.95	0.22	Bright rim
TZW87-27a	4.66	0.22	TZW89-27a	4.73	0.21	TZW94-27a	4.51	0.20	TZW99-26b	4.75	0.22	TZW95-27a	5.17	0.22		TZW96-27a	5.33	0.22	
TZW87-28a	4.61	0.22	TZW89-27b	4.82	0.21	TZW94-28a	4.66	0.20	TZW99-28a	4.91	0.22	TZW95-27b	3.99	0.22	Bright rim	TZW96-27b	5.06	0.22	Bright rim
TZW87-29	4.59	0.22	TZW89-29a	4.99	0.21	TZW94-28b	4.55	0.20	TZW99-28b	4.64	0.22	TZW95-29a	5.10	0.22		TZW96-15b	4.83	0.22	Bright rim
TZW87-30	4.76	0.22	TZW89-29b	4.82	0.21	TZW94-30	4.51	0.20	TZW99-30	4.82	0.22	TZW95-29b	3.88	0.22	Bright rim	TZW96-19b	4.89	0.22	Bright rim
						TZW94-31	4.69	0.23	TZW99-31a	4.75	0.21	TZW95-31a	5.26	0.20		TZW96-31	4.78	0.19	Bright rim
						TZW94-32	4.84	0.23	TZW99-31b	4.90	0.21	TZW95-32a	4.96	0.20		TZW96-32	5.33	0.19	
						TZW94-33	4.58	0.23	TZW99-33	4.95	0.21	TZW95-33a	5.11	0.20		TZW96-33a	4.77	0.19	Bright rim
						TZW94-34	4.58	0.23	TZW99-34	4.69	0.21	TZW95-34	5.25	0.20		TZW96-34	5.40	0.19	
						TZW94-35	4.65	0.23	TZW99-35	4.82	0.21	TZW95-35a	5.25	0.20		TZW96-35a	5.38	0.19	
						TZW94-36	4.75	0.23	TZW99-36	4.92	0.21	TZW95-35b	3.85	0.20	Bright rim	TZW96-36a	5.41	0.19	
						TZW94-37	4.82	0.23	TZW99-37	4.91	0.21	TZW95-37a	5.19	0.20		TZW96-37	4.97	0.19	
						TZW94-38	4.71	0.23	TZW99-38	4.67	0.21	TZW95-37b	3.92	0.20	Bright rim	TZW96-38	5.41	0.19	
						TZW94-39	4.97	0.23	TZW99-39a	4.74	0.21	TZW95-39a	5.17	0.20		TZW96-39	5.25	0.19	
						TZW94-40	4.57	0.23	TZW99-39b	4.80	0.21	TZW95-39b	4.11	0.20	Bright rim	TZW96-40	5.42	0.19	
												Average (zoned domain)	5.05	0.31		Average (zoned domain)	5.23	0.29	
												Average (bright rim)	3.82	0.37		Average (bright rim)	4.90	0.21	
Average	4.74	0.24	Average	4.77	0.29	Average	4.62	0.35	Average	4.81	0.28	Total average	4.74	1.12		Total average	5.17	0.38	

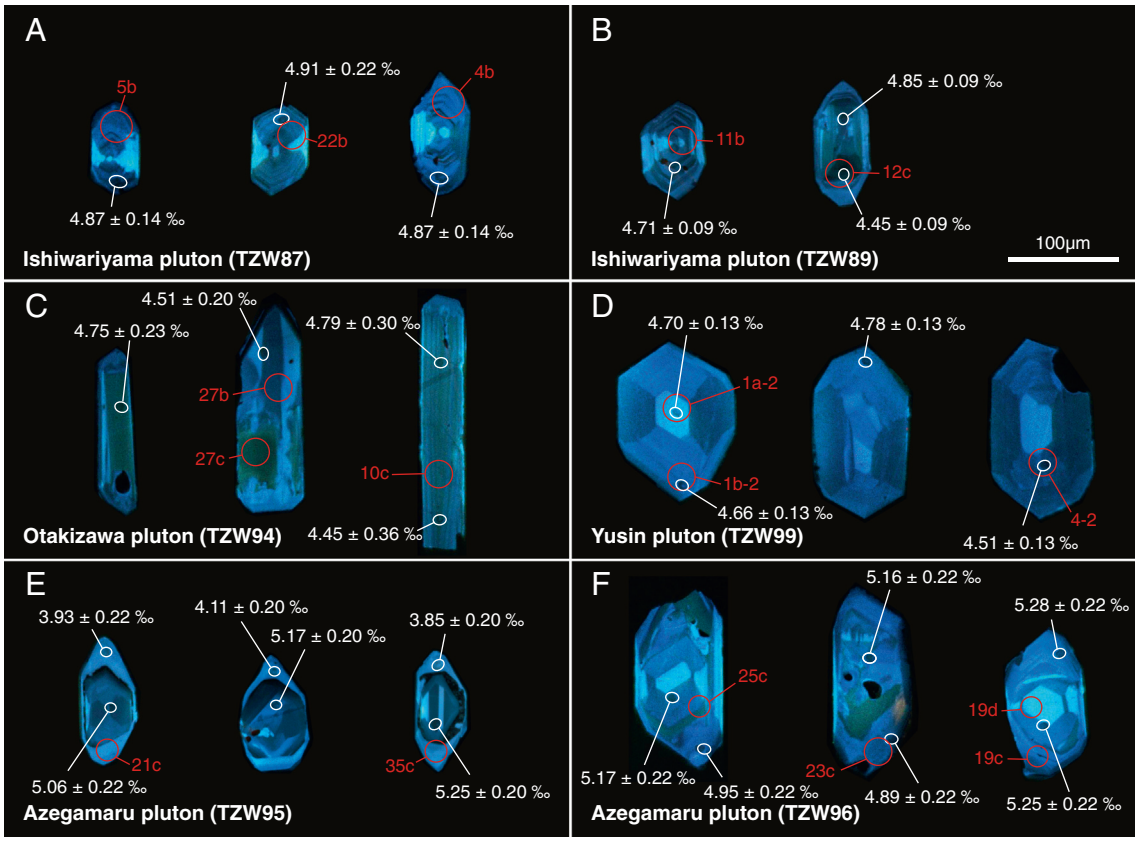

Fig. 3. Cathodoluminescence images of zircons separated from tonalities. Red and white circles represent analytical spots by LA-ICP-MS and SIMS, respectively. Zircons from the tonalite are euhedral shapes, and display oscillatory zoning, sector zoning and banded textures (see text for the details).(For interpretation of the references to color in this figure legend, the reader is referred to the web version of this article.)

ratios of cores show a prominent peak at *ca.* 5.1‰ (Table 1 and Fig. 4). We could not determine the $\delta^{18}O$ composition of the zircons with bright rims in the Ishiwariyama pluton due to their small dimension.

4.4. Trace element composition

Results for the trace element composition in the zircon are shown in Table S3 in the Supplementary information, and C1 chondrite-normalized rare earth element (REE) patterns are shown in Fig. 5. All of zircons display heavy rare earth element (HREE) enriched patterns which is characteristic of igneous zircons (e.g., Hoskin and Ireland, 2000). Almost all zircons display uniformly positive Ce anomaly and negative Eu anomaly; the latter reflects degree of crystallization of plagioclases before zircon formation (e.g., Hoskin and Schaltegger, 2003). In addition, almost all zircons display small Yb enrichment which is also shown in a previous work for Tanzawa Tonalites (Tani et al., 2010) but not in typical igneous zircons (e.g., Hoskin and Ireland, 2000). Bright rims, with lower $\delta^{18}O$ values, display lower REE contents and larger negative Eu anomalies than those in zoning region within each grain (Figs. 3E, F, and 5).

The U–Pb age of the zircons are also shown in Table S3. From the Ishiwariyama, Yusin and Azegamaru plutons, we obtained the similar U–Pb ages to the previous studies (Tani et al., 2010; Suzuki et al., 2014). Our U–Pb zircon age from the Otakizawa pluton (Stage 3) is the first to be reported (*ca.* 5.0 Ma), and is similar or slightly older than the igneous ages of the Yusin and Azegamaru plutons (Stage 4). This result supports the relative chronology based on outcrop observation for the intrusions (Takita, 1974).

5. Discussion

5.1. Comparison with oxygen isotope composition in whole rock

$\delta^{18}O$ values in whole rock of the TTP have previously been reported by Ishihara and Matsuhisa (2005). The $\delta^{18}O$ values of zircon cores obtained from this study are shown in Fig. 6, with the values acquired from whole rock analyses of the TTP (4.8 to 5.7‰; Ishihara and Matsuhisa, 2005) and the mantle value deduced from peridotite xenolith (5.4 to 5.8‰; Ionov et al., 1994).

To enable comparison between the zircons $\delta^{18}O$ values and whole rocks $\delta^{18}O$ values, we determined equivalent whole rock values for specific whole rock SiO_2 contents (Table S2), using measured zircon $\delta^{18}O$ values (Table 1) and the following equation (Lackey et al., 2008):

$$\Delta^{18}O_{(WR-Zrc)} \approx 0.0612 \times SiO_2 \text{ content (wt.\%)} - 2.50 \text{ (‰)}.$$

The equation is proposed for oxygen isotope fractionation between zircon (Zrc) and whole rock (WR), based on $\delta^{18}O$ analyses for zircons and the SiO_2 content of host granites in Sierra Nevada Batholith. The calculated whole rock values range from 6.51‰ to 6.74‰ (Fig. 6).

Although there are some uncertainties to apply this equation to the tonalites in the TTP, because of the different mineral assemblage from that of the granitoids in Sierra Nevada Batholith, if the equation is applicable, the $\delta^{18}O$ values of the melt calculated from zircons are *ca.* 1‰ higher than the measured whole rock $\delta^{18}O$ values reported by the previous study (4.8–5.7‰; Ishihara and Matsuhisa, 2005). $\delta^{18}O$ value in whole rock is usually modified by crystal fractionation processes (e.g., Matsuhisa, 1979; Taylor and Sheppard, 1986; Eiler, 2001; Lackey

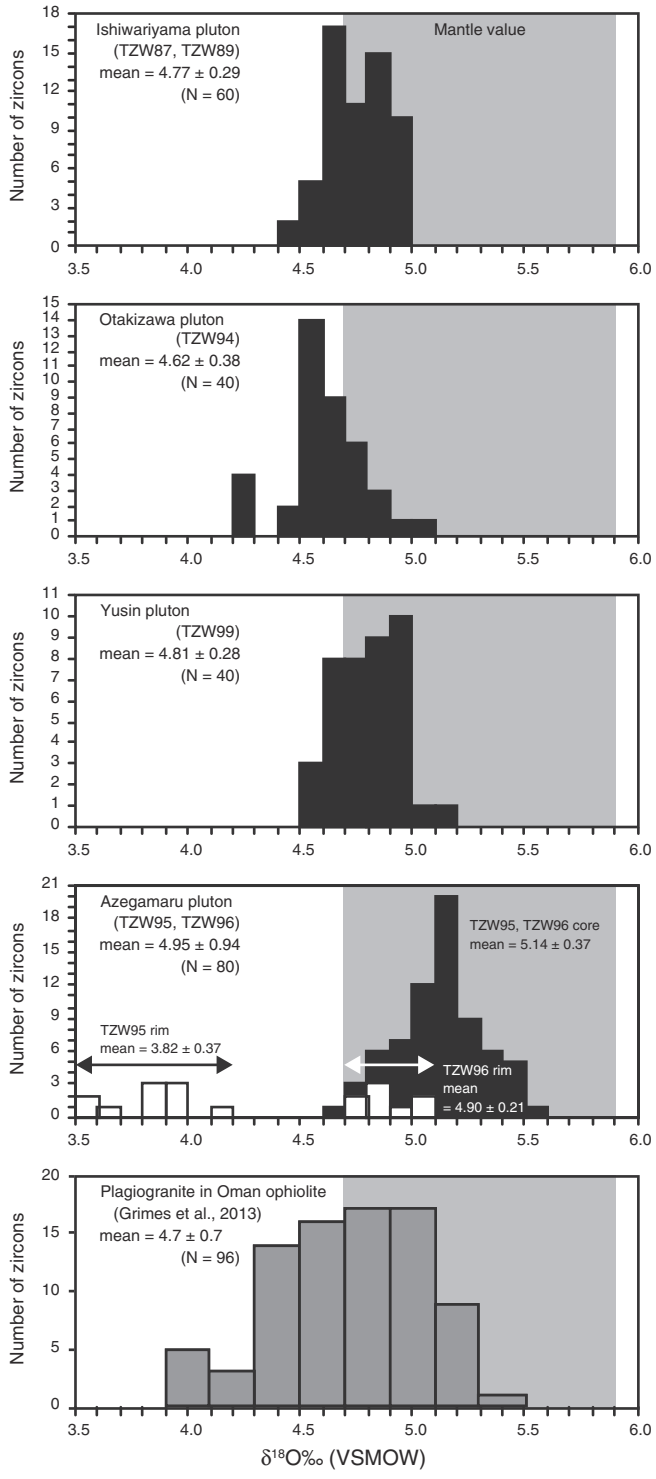

Fig. 4. Frequency diagrams for oxygen isotope ratios in zircons. Black and white squares represent oxygen isotope data from core and bright homogenous rim, respectively. Gray area corresponds to the range of oxygen isotope value of mantle deduced from zircons in kimberlite (Valley et al., 1998). For comparison, frequency of oxygen isotope ratios in zircons from plagiogranite in Oman ophiolite (Grimes et al., 2013) is also shown in the lowest diagram.

et al., 2008) and by alteration during later processes, and may not directly reflect the $\delta^{18}O$ value of source rocks (e.g., Eiler et al., 2000; Ito et al., 2003). The difference between calculated and measured whole rock values may be caused from alteration by surface water to measured whole rock values. On the other hand, the $\delta^{18}O$ value of zircon is nearly constant irrespective of SiO_2 content (Valley et al., 1994; Lackey et al., 2008) and usually not affected by surface water after crystallized (e.g. Cherniak and Watson, 2003). Therefore, it is suggested that zircons in this study probably preserve the $\delta^{18}O$ of the protolith better than the whole rock $\delta^{18}O$ values.

5.2. Oxygen isotope composition of zircons in the Tanzawa Tonalite

The $\delta^{18}O$ values in zircons from the Ishiwariyama, Otakizawa and Yusin plutons range from 4.1 to 5.1‰, which is slightly lower than mantle range constrained from $\delta^{18}O$ of zircons in kimberlite ($\delta^{18}O = 5.3 \pm 0.6$‰; Valley et al., 1998) and those in oceanic crust ($\delta^{18}O = 5.2 \pm 0.5$‰; Grimes et al., 2011). Furthermore, the bright rim of some zircons from the Azegamaru pluton (TZW95) generally displays lower $\delta^{18}O$ value than that of the zoned cores (Table 1 and Figs. 3 and 4). The differences of $\delta^{18}O$ within single zircon grains indicate that the zoned core and the bright rim formed under different conditions. The U–Pb ages of the bright rims are almost the same as those of the cores through the LA-ICP-MS analysis (Table S3), indicating that the core and rim formed penecontemporaneously within error of the analysis.

Oxygen isotope compositions in igneous minerals change by the difference of $\delta^{18}O$ value in protolith having undergone partial melting and/or difference of crystallization temperature, because $\Delta^{18}O_{mineral-mineral}$ values increase with decreasing temperature (e.g., Eiler, 2001). The effect of crystallization temperature is typically not so large (less than 1‰ for zircon), however, it must be considered in this case. Grimes et al. (2011) calculated the change in $\delta^{18}O$ in minerals at different crystallization temperatures from identical melts and applied the result to $\delta^{18}O$ value of zircons from oceanic crust. Fig. 7 shows the results for individual zircons and calculated curves representing relationships between $\delta^{18}O$ value and crystallization temperature. Results from Grimes et al. (2011) indicate that mantle zircons would be expected to plot on this curve in Fig. 7. Crystallization temperatures of zircons in the Azegamaru and Yusin plutons were calculated using the Ti thermometer (*ca.* 700–800 °C; Tani et al., 2010). We assume that the zircon cores in the Azegamaru and Yusin had similar crystallization temperatures to those in previous study (Fig. 7). Comparison of our data with previous work shows that results from Azegamaru pluton plot on the calculated curve but those from Yusin pluton lie outside the range of the curve (Fig. 7).

Zircons with bright rims from Azegamaru pluton have low $\delta^{18}O$ values compared to core (Fig. 3E). Genesis of the bright rim can be interpreted by the following two hypotheses: (1) The rim was crystallized from a suite of magma which crystallized core of the zircon. In this case, low $\delta^{18}O$ value at the bright rim can be well explained by a decreasing of crystallization temperature along with cooling of the magma (see following interpretation); and (2) The rim was latterly modified and/or altered by low $\delta^{18}O$ magma or hydrothermal fluids.

Although there is no constraint for the formation temperature of the rim, it is likely that during cooling of the magma the rim was formed at lower temperature than the core. The bright rim of the zircons from the Azegamaru pluton (TZW95) shows systematically lower REE concentrations and larger negative Eu anomalies compared to the zoned domains of the zircons (Fig. 5). The larger negative Eu anomaly in the bright rim suggests that the rim crystallized from, or reacted with, more differentiated magma compared to the zoned domain. Hypothetically assuming the crystallization temperature of the rim is similar to that of the rims of plagiogranite in previous study (*ca.* 625 °C; Grimes et al., 2011), the results from the rim plot on the same curve as the core of zircon from Azegamaru pluton (Fig. 7). These lines of evidence support former hypothesis that the bright rim of zircon from the Azegamaru pluton was formed at the late stage of crystallization (low temperature condition) and yields lower $\delta^{18}O$ value.

Latter hypothesis, modification and/or alteration by additional low $\delta^{18}O$ magma or hydrothermal fluids, is supported by eroded signature of internal structures by bright rim in the CL observation (Fig. 3E). Recrystallization of zircon in solid-state also modifies trace element

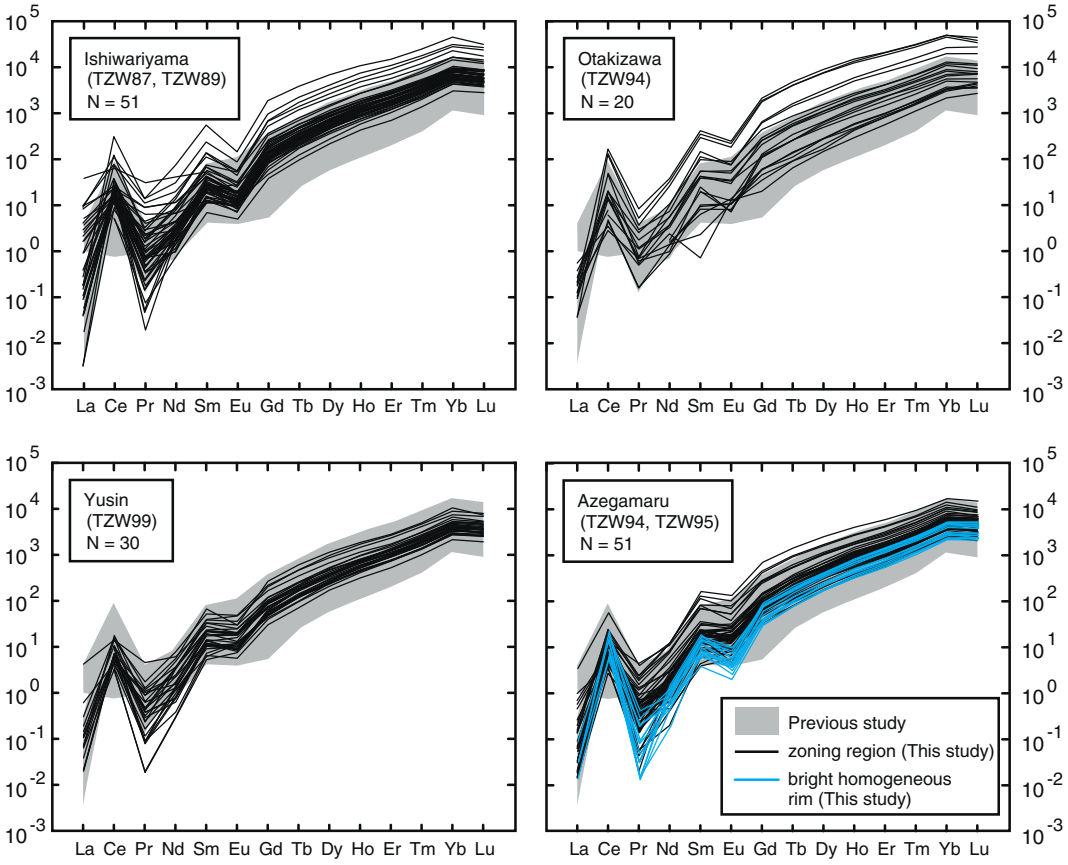

Fig. 5. Chondrite-normalized REE patterns of zircons from each pluton. Black and blue lines represent data from core and bright homogenous rim, respectively. Gray region shows REE patterns of zircons from previous studies in Ishiwariyama, Mizunoki and Azegamaru plutons (Tani et al., 2010; Suzuki et al., 2014). Chondrite data are from McDonough and Sun (1995).(For interpretation of the references to color in this figure legend, the reader is referred to the web version of this article.)

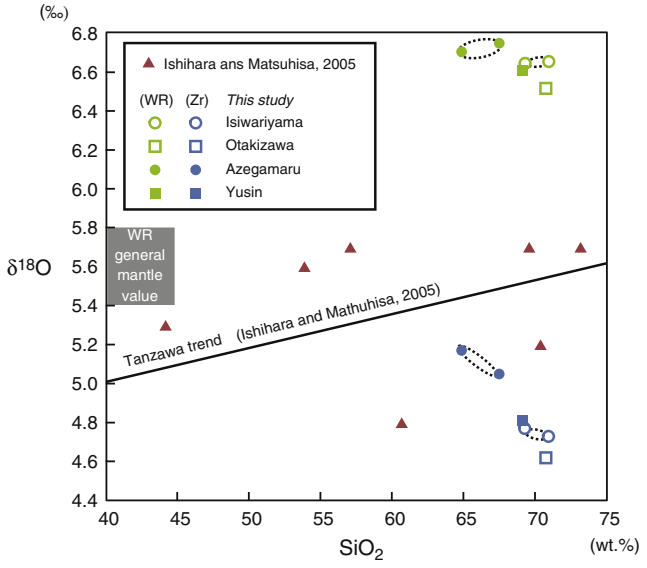

Fig. 6. Isotopic and elemental cross-plot for $\delta^{18}O$ value vs. SiO_2 content. Blue symbols represent average zircon $\delta^{18}O$ values for each tonalite sample. Green symbols represent whole rock $\delta^{18}O$ values calculated from the zircon $\delta^{18}O$ values and isotope fractionation factor between whole rock and zircon (Lackey et al., 2008). Measured whole rock $\delta^{18}O$ values (red triangles) and "Tanzawa trend" are from Ishihara and Matsuhisa (2005). Gray region represents whole rock mantle value estimated from peridotite xenolith (Ionov et al., 1994).(For interpretation of the references to color in this figure legend, the reader is referred to the web version of this article.)

composition in the zircon. For example, recrystallized zircons have flatter LREE and concave HREE patterns than igneous zircons (e.g. Hoskin and Ireland, 2000). The bright rims in this study, however, show no development of such patterns compared to those in core (Fig. 5). In addition, if modification by low $\delta^{18}O$ magma occurs, it is assumed that such magma precipitates some zircons whose cores have low $\delta^{18}O$ equivalent to the rim. Nonetheless we could not detect such low $\delta^{18}O$ values from the core in any zircon. This suggests that the Azegamaru Pluton is unaffected by large-scale alteration by low $\delta^{18}O$ magma or hydrothermal fluids which modify trace element pattern. Whatever the cause, only $\delta^{18}O$ value of zoned domain at core is used for source rock estimation in the following discussion, since the zoned domain shows similar CL texture and REE signature to zircons from other plutons (Figs. 3 and 5).

Compared to the $\delta^{18}O$ in zircons from this study and Grimes et al. (2011), zircon cores from Azegamaru pluton plotted on calculated gray curve (Fig. 7), indicating that its protolith was dominated by material equilibrated with mantle. On the other hand, if we assume similar crystallization temperature (*ca.* 700–800 °C) to zircons from Ishiwariyama and Otakizawa plutons, the results from Ishiwariyama, Otakizawa and Yusin plutons are plotted on out of the range of the calculated curve. This suggests that zircons with lower $\delta^{18}O$ values than mantle, cannot be explained only by crystallization temperature. This suggests that these plutons were derived from source rock which contain non-mantle-like component.

5.3. Protolith of Tanzawa Tonalite

Based on relatively high Th/Nb ratios in zircons, Tani et al. (2010) suggested that sedimentary material from the Honshu arc was involved

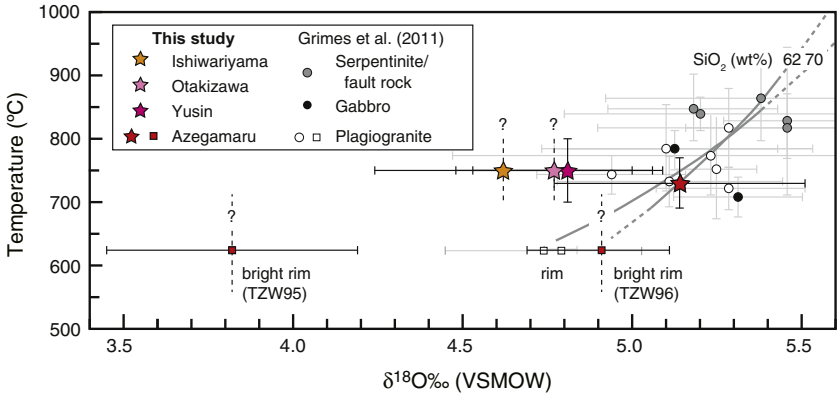

Fig. 7. Cross-plot showing relationship between $\delta^{18}O$ in minerals and crystallization temperature. Black-and-white dots represent analytical data from Grimes et al. (2011). Solid gray curves showing shift of $\delta^{18}O$ in minerals crystallized from mantle-like melt at various temperature ranges. The solid gray curves are positioned assuming an equilibrium with $\delta^{18}O_{diopside} = 5.3‰$ at 800 °C (see Grimes et al. (2011) for the details). Colored symbols represent results of this study. Crystallization temperatures of the Yusin and Azegamaru plutons (*ca.* 700–800 °C) were calculated by Tani et al. (2010) using Ti-in-zircon thermometer (Watson et al., 2006) and calibrations from Ferry and Watson (2007), assuming $a_{TiO2} = 0.7$ and $a_{SiO2} = 1$. The error bars represent 2SD. On the other hand, there is no constraint for crystallization temperature of Ishiwariyama and Otakizawa plutons.(For interpretation of the references to color in this figure legend, the reader is referred to the web version of this article.)

in the genesis of the Tanzawa tonalitic magma. The zircons in the Tanzawa Tonalite have slightly lower or similar $\delta^{18}O$ values compared to the mantle $\delta^{18}O$ value (Fig. 4; Valley et al., 1998; Page et al., 2007). In general, sediments through reaction with surface water at low temperature have high $\delta^{18}O$ values (from *ca.* 10 to 25‰; e.g., Gregory and Taylor, 1981). In this study, although Th/Nb ratios in the zircons vary from 13 to 784 (Table S3), the $\delta^{18}O$ in them are uniformly low values ranging from 4.2 to 5.6‰ (Fig. 4). There is no correlation between Th/Nb ratios and $\delta^{18}O$ values (Tables 1 and S3), and low $\delta^{18}O$ values in the zircons suggest insignificant involvement of sedimentary material.

As discussed above, the lower $\delta^{18}O$ values of zircons from the Ishiwariyama, Otakizawa and Yusin plutons suggest that their parent rocks had slightly lower $\delta^{18}O$ values than the mantle (Fig. 4). Lower $\delta^{18}O$ value than the mantle can be caused by reaction with meteoric water, which has significantly low $\delta^{18}O$ value, or by hydrothermal alteration with surface water. In the latter case, the small isotope fractionation between water and rock at high temperature results in the low $\delta^{18}O$ value of hydrothermally altered rock (e.g., Muehlenbachs, 1986). As the Tanzawa Tonalite is believed to have been generated by partial melting of island arc lower crust (Nakajima and Arima, 1998) and to have intruded basaltic–andesitic pyroclastic rocks (Tanzawa Group; Fig. 1; Aoike et al., 1997), candidates for cause of the low $\delta^{18}O$ values are; (1) dehydration from Pacific plate to the IBM sub-arc mantle, (2) contamination/reaction of meteoric water and/or hydrothermal alteration in the Tanzawa Group, and (3) existence of former lower oceanic crust in the IBM arc crust.

We first consider heterogeneity of $\delta^{18}O$ value in the mantle, because most of the arc lower crust in IBM arc and the basaltic–andesitic rocks of Tanzawa Group were generated by partial melting of mantle. $\delta^{18}O$ values of MORB, which reflects the composition of the depleted upper mantle, are extremely homogeneous ($5.7 \pm 0.2‰$; Ito et al., 1987; Eiler, 2001). By contrast, peridotite xenoliths in alkali basalts and eclogite xenoliths in kimberlite show a wide range of $\delta^{18}O$ values (Garlick et al., 1971; Javoy, 1980; Harmon et al., 1987; Ongley et al., 1987; Kempton et al., 1988; Neal et al., 1990; Pearson et al., 1991; Eiler, 2001). During dehydration of subducting plates anomalous amounts (e.g., >5 wt.%) of low $\delta^{18}O$ fluid may be transferred to the mantle wedge. This might cause a slight decrease in the $\delta^{18}O$ value of the mantle wedge. However, laser-fluorination analyses for olivine and fresh glass in lava from island arcs show similar or higher $\delta^{18}O$ values compared to that of MORB (Smith et al., 1996; Thirlwall et al., 1996; Macpherson and Mattey, 1997; Macpherson et al., 1998; Eiler et al., 2000). In the Mariana arc, the $\delta^{18}O$ values of melt estimated from olivine (Eiler et al., 2000) and clinopyroxyne (Ito et al., 2003) in basaltic lavas, which are in equilibrium with upper-mantle peridotites and MORB, show narrow range around 5.6–5.7‰. These lines of evidence suggest that the heterogeneity of mantle under the IBM arc is unlikely to attribute to low $\delta^{18}O$ values in zircons from TTP, and supports the involvement of low $\delta^{18}O$ crustal material to the magma source.

A second possibility is that the cause of the low $\delta^{18}O$ values of the TTP is reaction of the Tanzawa Group with surface water. Both rocks which reacted with meteoric water (e.g., Wang and Eiler, 2008) and with seawater in high temperature (>200–300 °C; Muehlenbachs and Clayton, 1976) have lower $\delta^{18}O$ values than original rocks. In the Tanzawa Group, an unconformity estimated to be formed at *ca.* 8.6 Ma (Aoike, 1999) is only reported at boundary between Hayato subgroup and Susugaya subgroup. This means that the Tanzawa Group was only raised above sea level after the intrusion of the Ishiwariyama pluton (8.8–8.9 Ma; Tani et al., 2010). Thus, reaction between meteoric water and rocks of the Tanzawa Group probably did not occur before formation of the Ishiwariyama pluton. Substantially deep intrusion depth of the tonalite (6–7 km; Toriumi and Arai, 1986) also excludes the possibility of involvement with the meteoric water. Hydrothermal activity, on the other hand, may reach depth of ca. 7 km and it could cause reaction between seawater and rocks in high temperature (~350 °C) in volcanic front (e.g., Ishihbashi and Urabe, 1995). If large-scale hydrothermal alteration causing a decrease of $\delta^{18}O$ in the TTP had occurred it should be recognized in the field, but no evidence of such an intense hydrothermal activity has been reported in the Tanzawa Group. Thus the influence of the surface water is not a plausible cause of low $\delta^{18}O$ values in the tonalites, especially in the Ishiwariyama pluton.

Third possibility is the existence of the ancient oceanic crust in the arc lower crust beneath the TTP. In principle, island arc crust is formed on oceanic crust at first by initiation of plate-subduction (Fig. 8A). Therefore, proto-island arc crust probably contains a component of former oceanic crust. The $\delta^{18}O$ value of hydrothermally altered gabbros at lower oceanic crustal level, where reactions with sea water at high temperatures occur (above *ca.* 400 °C; e.g., Muehlenbachs, 1986), is reported as ranging from 0 to 6‰, and typically ranging from 4 to 5‰, based on results from modern oceanic crust (e.g., Kempton et al., 1991; Lecuyer and Gruau, 1996) and ophiolite (e.g., Gregory and Taylor, 1981). This suggests that the low zircon $\delta^{18}O$ values in the Tanzawa Tonalites could be produced by melting of island arc lower crust including former lower oceanic crust (Fig. 8). The existence of the former oceanic crust in the island arc lower crust has been implied based on whole rock REE patterns of mafic enclaves in the TTP (Suzuki et al., 2014). Some mafic enclaves have flat N-MORB normalized REE patterns,

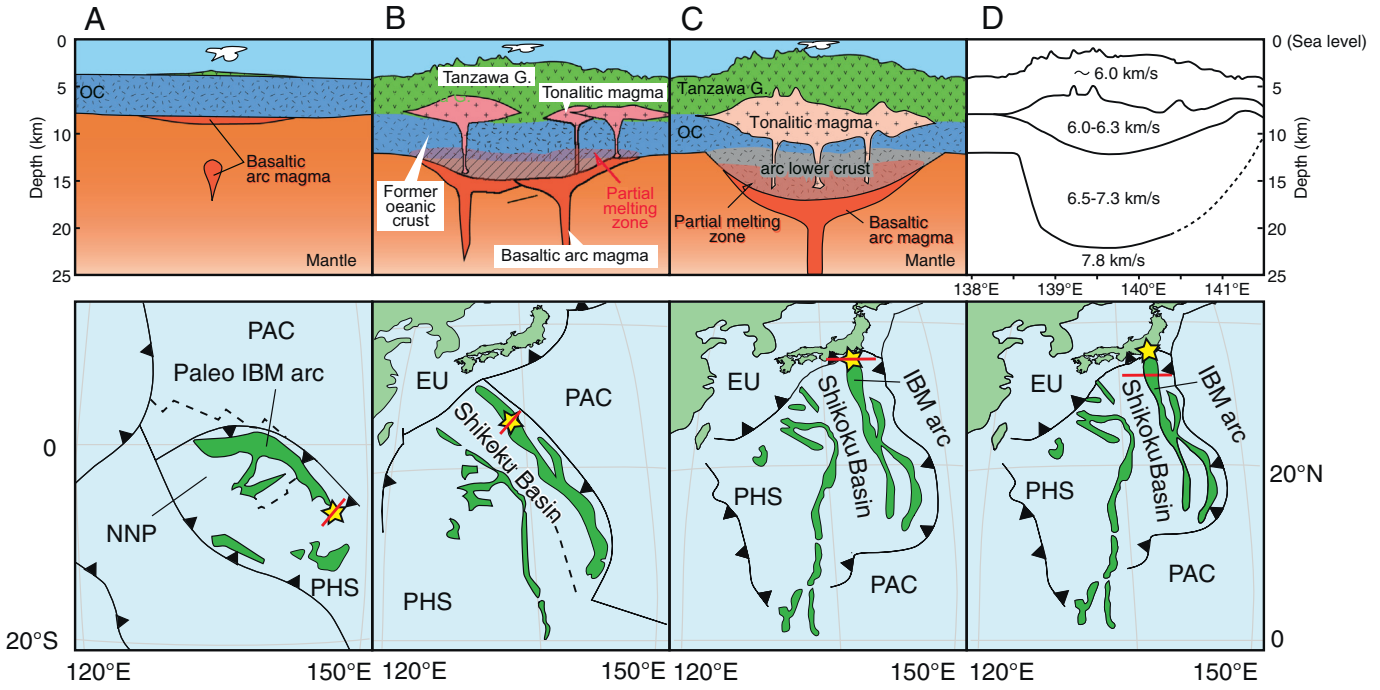

Fig. 8. Schematic cross sections of the proto Tanzawa Block, which displays the formation model of the TTP (above) and paleogeographical maps displaying the spatial location of the IBM arc through time (modified from Tatsumi et al., 2008; below). The transect line for the cross section (solid red line) and location of the (proto) Tanzawa Block (star symbol) are also shown. NNP, North New Guinea Plate. (A) Initial arc crust was formed on oceanic crust (OC) before 43 Ma. (B) Basaltic magma of Tanzawa group erupted after 17 Ma. Arc lower crust had been continuously evolved by basaltic arc magmatism at proto-IBM arc. (C) Intrusions of TTP occurred at 4–9 Ma by partial melting of the arc lower crust including former oceanic crust. Cross section of (A)–(C) are based on the present-day seismic observation of northern IBM arc (D); modified from Suyehiro et al. (1996).(For interpretation of the references to color in this figure legend, the reader is referred to the web version of this article.)

suggesting that they originated from arc lower crust with MORB-like compositions. Some of these MORB-like rocks are most likely preserved at depth within arcs.

Of the three possibilities, the third is considered to be most plausible for low $\delta^{18}O$ values in the TTP especially for the Ishiwariyama pluton. Thus, we conclude that ancient oceanic crustal material, such as hydrothermally altered gabbro, was a component of island arc lower crust at least when the Ishiwariyama pluton was generated (9 Ma; Fig. 8). Recently, Grimes et al. (2013) reported similar $\delta^{18}O$ range of zircons from plagiogranite in 8 ophiolites, especially in Oman ophiolite (4.7 ± 0.7‰; Fig. 4). The low $\delta^{18}O$values in zircons from plagiogranite were interpreted to be caused by re-melting of hydrothermally altered oceanic crust near the dike-gabbro transitional zone. The similarity of oxygen isotope ratio in zircons also suggests that the Tanzawa Tonalite including the Ishiwariyama, Mizunoki and Yusin plutons has their roots in hydrothermally altered gabbro in former oceanic crust.

5.4. Implication: residence time of oceanic crust in arc lower crust

It is generally suggested that the former oceanic crust has been modified or disappeared in the mature continental lower crust. The higher $\delta^{18}O$ values of some granulite xenoliths (5.4 to 13.5‰; Fowler and Harmon, 1990; Kempton et al., 1991) relative to the mantle value (5.4 to 5.8‰; Ionov et al., 1994) support this interpretation. Although it is commonly inferred that the former oceanic crust in the arc lower crust is modified during its evolution, the timing of modification and disappearance is not well established.

Two contrasting models for the evolution from the oceanic crust to the island arc crust have been proposed based on seismic observations and geochemistry, i.e., (1) former oceanic crust remains as part of the arc lower crust even after felsic magma (granodiorite) generation by partial melting of the arc lower crust (e.g., Kuno, 1968), and (2) the oceanic crust is replaced by incipient basaltic arc magmatism in short time (e.g. Tatsumi et al., 2008). In the Aleutian arc, northwestern margin of the Pacific Ocean, existence of ~10 km thick former oceanic crust within island arc crust is suggested based on seismic observations (Holbrook et al., 1999; Shillington et al., 2004) and radiogenic Nd isotopic ratios of volcanic rocks and xenoliths (Kay et al., 1986). As the Aleutian arc crust was formed at 55–50 Ma (Scholl et al., 1987), it is likely that the former oceanic crust remains in the Aleutian arc over 50 million years. However, arguments based on the geological evidence have been limited due to the difficulty of obtaining lower crustal material from the arc. Furthermore, the case of the Aleutian arc may not able to be applied to other island arcs which have thick (~5 km) middle felsic crust like the IBM arc (Suyehiro et al., 1996; Takahashi et al., 2007), because the seismic structure of the Aleutian arc shows lack of middle layer with felsic composition.

In the case of the TTP, the collision between the Tanzawa Block and the Honshu arc is an important problem. If the protolith of the TTP was changed during the collision, the TTP does not represent the middle crust of the intra oceanic IBM arc. The Ishiwariyama pluton (8–9 Ma; Tani et al., 2010) and other plutons (4–5 Ma; Tani et al., 2010) were formed at the timing before and during the collision (3.8–6.8 Ma; Yamamoto and Kawakami, 2005), respectively. However, the whole rock compositions (Table S2; Takahashi et al., 2004), oxygen isotope ratios and REE patterns of zircons show no significant difference among the Ishiwariyama, Otakizawa and Yusin plutons (Figs. 4 and 5). These data suggest that the collision between the Tanzawa Block and the Honshu arc probably did not change the protolith that was melted to produce the TTP. Furthermore, the Otakizawa and Yusin plutons also seemed to contain a component of ancient oceanic crust as their protoliths, based on their slightly lower zircon $\delta^{18}O$ values (Table 1; Fig. 4).

These data suggest that ancient oceanic crust had (partially) existed in the IBM arc crust from the initial arc generation until intrusion of the Yusin pluton (Fig. 8). The age of the lower crust beneath Tanzawa Tonalite is suggested to be >43 Ma based on zircon U–Pb age from mafic enclave in the TTP (Suzuki et al., 2014). This age constraint on arc lower crust suggests that former oceanic crust existed for at least *ca.* 40 million years after the initial arc generation, especially in the IBM arc. This is the first geochemically based estimate for the longevity of the former oceanic crust within the arc lower crust. By constraining residence time of former oceanic crust in the arc system, our study has enabled the evolutionary processes responsible for the transition from oceanic crust to island arc crust to be better constrained.

6. Conclusion

Principal conclusions from our study are as follows:

(1) $\delta^{18}O$ values of zircons from the Tanzawa Tonalite are slightly lower or similar to mantle $\delta^{18}O$ values.
(2) These low $\delta^{18}O$ values are interpreted to reflect involvement of ancient oceanic crustal material in the arc crust beneath the Tanzawa Tonalitic Pluton.
(3) Based on estimation of formation age of arc lower crust by zircon U–Pb age in mafic enclaves (Suzuki et al., 2014), this ancient oceanic crustal component of the arc architecture possibly existed for least 40 million years from initial arc generation to emplacement of the TTP suite.

Supplementary data to this article can be found online at http://dx.doi.org/10.1016/j.lithos.2015.04.005.

Acknowledgments

We are grateful to Prof. J. W. Valley, N. Kita, and J. Kern for helpful discussions and kind support in oxygen isotope analysis at the University of Wisconsin-Madison. We are also grateful to Prof. K. D. Collerson for correcting our English grammar. KS appreciates Prof. K. Hirose for the support to realize the analysis at the University of Wisconsin-Madison. Prof. C. Grimes and anonymous reviewer gave many constructive and helpful comments, which improved quality of this manuscript. Prof. S.-L. Chung, the editor of this journal, handled this manuscript. This work was supported by grants for the Global COE Program, "From the Earth to "Earths"", from the Ministry of Education, Culture, Sports, Science and Technology, Japan, and JSPS KAKENHI grant number 14J12001.

References

Aoike, K., 1999. Tectonic evolution of the Izu Collision Zone. Research report of the Kanagawa Prefectural Museum. Natural History 9, 111–151.
Aoike, K., Arima, M., Koike, T., 1995. Magnesian andesite exposed in the eastern Tanzawa Massif. Petrology, and Economic GeologistsAbstract Program 1994 annual Meeting Japan Association of Mineralogy, Sendai, Japan, p. 14.
Aoike, K., Kadota, M., Suekane, T., Aikawa, K., Matsushima, Y., Kawate, S., Yamashita, H., Umezawa, S., Imanaga, I., 1997. Geology of the Tanzawa Mountains and surrounding area. Comprehensive research report of natural environment in the Tanzawa Mountains. Kanagawa Prefecture. Department of Environment, pp. 24–63.
Cherniak, D.J., Watson, E.B., 2003. Diffusion in zircon. In: Hanchar, J.M., Hoskin, P.W.O. (Eds.), Zircon. Reviews in Mineralogy and Geochemistry. vol. 53. Mineralogical Society of America, Washington, D.C, pp. 113–143.
Corfu, F., Hanchar, J.M., Hoskin, P.W.O., Kinny, P., 2003. An atlas of zircon textures. In: Hanchar, J.M., Hoskin, P.W.O. (Eds.), Zircon. Reviews in Mineralogy and Geochemistry. vol. 53. Mineralogical Society of America, Washington, D.C, pp. 469–500.
Cosca, M.A., Arculus, R.J., Pearce, J.A., Mitchell, J.G., 1998. $^{40}Ar/^{39}Ar$ and K–Ar geochronological age constraints for the inception and early evolution of the Izu–Bonin–Mariana arc system. Island Arc 7, 579–595.
Eggins, S.M., Kinsley, L.P.J., Shelley, J.M.G., 1998. Deposition and element fractionation processes during atmospheric pressure laser sampling for analysis by ICP-MS. Applied Surface Science 127, 278–286.
Eiler, J.M., Crawford, A., Elliott, T., Farley, K.A., Valley, J.W., Stolper, E.M., 2000. Oxygen isotope geochemistry of oceanic-arc lavas. Journal of Petrology 41, 229–256.
Eiler, J.M., 2001. Oxygen isotope variations of basaltic lavas and upper mantle rocks. In: Valley, J.W., Cole, D.R. (Eds.), Stable Isotope Geochemistry. Reviews in Mineralogy and Geochemistry. 43. Mineralogical Society of America, Washington, D.C, pp. 319–364.
Ferry, J.M., Watson, E.B., 2007. New thermodynamic models and revised calibrations for the Ti-in-zircon and Zr-in-rutile thermometers. Contributions to Mineralogy and Petrology 154, 429–437. http://dx.doi.org/10.1007/s00410-007-0201-0.
Fountain, D.M., Salisbury, M.H., 1981. Exposed cross-sections through the continental crust: implications for crustal structure, petrology, and evolution. Earth and Planetary Science Letters 56, 263–277.
Fowler, M.B., Harmon, R.S., 1990. The oxygen isotope composition of lower crustal granulite xenoliths. In: Vielzeuf, D., Vidal, Ph. (Eds.), Granulites and Crustal Evolution. NATO ASI series vol. 311. Kluwer Academic Publishers, Netherlands, pp. 493–506.
Garlick, G.D., MacGregor, I.D., Vogel, D.E., 1971. Oxygen isotope ratios in eclogites from kimberlites. Science 172, 1025–1027.
Garrido, C.J., Bodinier, J.L., Burg, J.P., Zeilinger, G., Hussain, S.S., Dawood, H., Chaudhry, M.N., Gervilla, F., 2006. Petrogenesis of mafic garnet granulite in the lower crust of the Kohistan paleo-arc complex (Northern Pakistan): implications for intra-crustal differentiation of island arcs and generation of continental crust. Journal of Petrology 47, 1873–1914.
Gregory, R.T., Taylor, H.P., 1981. An oxygen isotope profile in a section of cretaceous oceanic crust, Samail Ophiolite, Oman: evidence for $\delta^{18}O$ buffering of the oceans by deep (>5 km) seawater-hydrothermal circulation at Mid-Ocean Ridges. Journal of Geophysical Research 86, 2737–2755.
Grimes, C.B., Ushikubo, T., John, B.E., Valley, J.W., 2011. Uniformly mantle-like $\delta^{18}O$ in zircons from oceanic plagiogranites and gabbros. Contribution to Mineralogy and Petrology 161, 13–33. http://dx.doi.org/10.1007/s00410-010-0519-x.
Grimes, C.B., Ushikubo, T., Kozdon, R., Valley, J.W., 2013. Perspectives on the origin of plagiogranite in ophiolites from oxygen isotopes in zircon. Lithos 179, 48–66.
Harmon, R.S., Hoefs, J., Wedepohl, K.H., 1987. Stable isotope (O, H, S) relationships in tertiary basalts and their mantle xenoliths from the Northern Hessian Depression, W. Germany. Contribution to Mineralogy and Petrology 95, 350–369.
Hirata, T., Iizuka, T., Orihashi, Y., 2005. Reduction of mercury background on ICP-mass spectrometry for in situ U–Pb age determinations of zircon samples. Journal of Analytical Atomic Spectrometry 20, 696–701.
Holbrook, W.S., Lizarralde, D., McGeary, S., Bangs, N., Diebold, J., 1999. Structure and composition of the Aleutian island arc and implications for continental crustal growth. Geology 27, 31–34.
Hoskin, P.W.O., Ireland, T.R., 2000. Rare earth element chemistry of zircon and its use as a provenance indicator. Geology 28, 627–630.
Hoskin, P.W.O., Schaltegger, U., 2003. The composition of zircon and igneous and metamorphic petrogeneis. In: Hanchar, J.M., Hoskin, P.W.O. (Eds.), Zircon. Reviews in Mineralogy and Geochemistry. 53. Mineralogical Society of America, Washington, D. C, pp. 27–62.
Ionov, D.A., Harmon, R.S., France-Lanord, C., Greenwood, P.B., Ashchepkov, I.V., 1994. Oxygen isotope composition of garnet and spinel peridotites in the continental mantle: evidence from the Vitim xenolith suite, southern Siberia. Geochimica et Cosmochimica Acta 58, 1463–1470.
Ishihara, S., Matsuhisa, Y., 2005. Oxygen isotopic constraints on the geneses of the Late Cenozoic plutonic rocks of the Green Tuff Belt, Northeast Japan. Bulltin of the Geological Survey of Japan 56, 315–324.
Ishihara, S., Kanaya, H., Terashima, S., 1976. Genesis of the Neogene granitoids in the fossa magna region in Japan. Marine Sciences Monthly. 8 pp. 523–528.
Ishihbashi, J., Urabe, T., 1995. Hydrothermal activity related to arc–backarc magmatism in the Western Pacific. In: Taylor, B. (Ed.), Backarc basins: tectonics and magmatism. Plenum Press, pp. 451–495.
Ishizaka, K., Yanagi, T., 1977. K, Rb and Sr abundances and Sr isotopic composition of the Tanzawa granitic and associated gabbroic rocks, Japan: low-potash island arc plutonic complex. Earth and Planetary Science Letters 33, 345–352.
Ishizuka, O., Kimura, J., Li, Y.B., Stern, R.J., Reagan, M.K., Taylor, R.N., Ohara, Y., Bloomer, S.H., Ishii, T., Hargrove III, U.S., Haraguchi, S., 2006. Early stages in the evolution of Izu–Bonin arc volcanism: new age, chemical, and isotopic constraints. Earth and Planetary Science Letters 250, 385–401.
Ito, E., White, W.M., Göpel, C., 1987. The O, Sr, Nd and Pb isotope geochemistry of MORB. Chemical Geology 62, 157–176.
Ito, E., Stern, R.J., Douthitt, C., 2003. Insights into operation of the subduction factory from the oxygen isotopic values of the southern Izu–Bonin–Mariana Arc. The Island Arc 12, 383–397.
Javoy, M., 1980. $^{18}O/^{16}O$ and D/H ratios in high-temperature peridotites. Colloques internationaux Centre national de la recherche scientifique 272, 279–287.
Kawano, Y., Ueda, Y., 1966. K–A dating on the igneous rocks in Japan (IV) — Granitic rocks in northeastern Japan. Journal of Mineralogy, Petrology and Economic Geology 56, 41–55.
Kawate, S., Arima, M., 1998. Petrogenesis of the Tanzawa plutonic complex, central Japan: exposed felsic middle crust of the Izu–Bonin–Mariana arc. Island Arc 7, 342–358.
Kawate, S., Fujimaki, H., 1996. Strontium Isotope Composition of the Tanzawa Plutonic Rocks in the Izu–Bonin Arc. Japan Earth and Planetary Science Joint Meeting, Abstracts, Osaka, Japan, p. 703.
Kay, R.W., Rubenstone, J.L., Kay, S.M., 1986. Aleutian terranes from Nd isotopes. Nature 322, 605–609. http://dx.doi.org/10.1038/322605a0.
Kempton, P.D., Harmon, R.S., Stosch, H.-G., Hoers, J., Hawkesworth, C.J., 1988. Open-system O-isotope behavior and trace element enrichment in the sub-Eifel mantle. Earth and Planetary Science Letters 89, 273–287.
Kempton, P.D., Hawkesworth, C.J., Fowler, M.B., 1991. Geochemistry and isotopic composition of gabbros from layer 3 of the Indian Ocean crust, Hole 735B. In: Von Herzen RE Robinson, P.T., et al. (Eds.), Proceedings of the Ocean Drilling Program-Scientific Results. 118, pp. 127–141.

Kita, N.T., Ushikubo, T., Fu, B., Valley, J.W., 2009. High precision SIMS oxygen isotope analysis and the effect of sample topography. Chemical Geology 264, 43–57.
Kitamura, K., Ishikawa, M., Arima, M., 2003. Petrological model of the northern Izu–Bonin–Mariana arc crust: constraints from high-pressure measurements of elastic wave velocities of the Tanzawa plutonic rocks, central Japan. Tectonophysics 371, 213–221.
Kuno, H., 1968. Origin of Andesite and Its Bearing on the Island Arc Structure. Bulletin Volcanologique 32, 141–176.
Lackey, J.S., Valley, J.W., Chen, J.H., Stockli, D.F., 2008. Dynamic magma systems, crustal recycling, and alteration in the central Sierra Nevada batholith: the oxygen isotope record. Journal of Petrology 49, 1397–1426.
Lecuyer, C., Gruau, G., 1996. Oxygen and strontium isotope compositions of Hess Deep gabbros (Holes 894F and 894G): high-temperature interaction of seawater with the oceanic crust layer 3. Proceedings of the Ocean Drilling Program-Scientific Results. 147, pp. 227–234. http://dx.doi.org/10.2973/odp.proc.sr.147.014.1996.
Machida, S., Ishii, T., Kimura, J.-I., Awaji, S., Kato, Y., 2008. Petrology and geochemistry of cross-chains in the Izu–Bonin back arc: three mantle components with contributions of hydrous liquids from a deeply subducted slab. Geochemistry, Geophysics, Geosystems 9 (5), Q05002. http://dx.doi.org/10.1029/2007GC001641.
Macpherson, C.G., Mattey, D.P., 1997. Oxygen isotope variations in Lau Basin lavas. Chemical Geology 144, 177–194.
Macpherson, C.G., Gamble, J.A., Mattey, D.P., 1998. Petrology of Matthew and Hunter volcanos, south New Hebrides island arc (southwest Pacific). Journal of Volcanology and Geothermal Research 30, 1–27.
Matsuda, T., 1978. Collision of Izu–Bonin arc with central Honshu. Cenozoic tectonics of the Fossa Magna Japan. Journal of Physics of the Earth 26, S409–S421.
Matsuhisa, Y., 1979. Oxygen isotopic compositions of volcanic rocks from the East Japan island arcs and their bearing on petrogenesis. Journal of Volcanology and Geothermal Research 5, 271–296.
McDonough, W.F., Sun, S.S., 1995. The composition of the Earth. Chemical Geology 120, 223–253.
Mezger, K., 1992. Temporal evolution of regional granulite terranes: implications for the formation of lowermost continental crust article. In: Fountain, D.M., Arculus, R., Kay, R.W. (Eds.), Continental Lower Crust. Elsevier, Amsterdam, pp. 447–478.
Muehlenbachs, K., 1986. Alteration of the oceanic crust and the ^{18}O history of seawater. In: Valley, J.W., Taylor, H.P., O'Neil, J.R. (Eds.), Stable Isotopes in High Temperature Geological Processes, 16. Mineralogical Society of America, Washington, D.C., pp. 425–444.
Muehlenbachs, K., Clayton, R.N., 1976. Oxygen isotope composition of the oceanic crust and its bearing on seawater. Journal of Geophysical Research 81, 4365.
Müller, R.D., Roest, W.R., Royer, J.Y., Gahagan, L.M., Sclater, J.G., 1997. Digital isochrons of the world's ocean floor. Journal of Geophysical Research, Solid Earth 102, 3211–3214.
Nakajima, K., Arima, M., 1998. Melting experiments on hydrous low-K tholeiite: implications for the genesis of tonalitic crust in the Izu–Bonin–Mariana arc. Island Arc 7, 359–373.
Neal, C.R., Taylor, L.A., Davidson, J.R., Holden, P., Halliday, A.N., Nixon, P.H., Paces, T., Clayton, R.N., Mayeda, T.K., 1990. Eclogites with oceanic crustal and mantle signatures from the Bellsbank kimberlite, South Africa. 2. Sr, Nd, and O isotope geochemistry. Earth and Planetary Science Letters 99, 362–379.
Ongley, J.S., Basu, A.R., Kyser, T.K., 1987. Oxygen isotopes in coexisting garnets, clinopyroxenes, and phlogopites of Roberts Victor eclogites: implications for petrogenesis and mantle metasomatism. Earth and Planetary Science Letters 83, 80–84.
Page, F.Z., Fu, B., Kita, N.T., Fournelle, J., Spicuzza, M.J., Schulze, D., Schulze, D.J., Viljoen, F., Basei, M.A.S., Valley, J.W., 2007. Zircons from kimberlite: new insights from oxygen isotopes, trace elements, and Ti in zircon thermometry. Geochimica et Cosmochimica Acta 71, 3887–3903.
Pearce, J.G., Perkins, W.T., Westgate, J.A., Gorton, M.P., Jackson, S.E., Neal, C.R., Chenery, S.P., 1997. A compilation of new and published major and trace element data for NIST SRM 610 and NIST SRM 612 glass reference materials. The Journal of Geostandards and Geoanalysis 21, 115–144.
Pearson, D.G., Davies, G.R., Nixon, P.H., Greenwood, P.B., Mattey, D.P., 1991. Oxygen isotope evidence for the origin of pyroxenites in the Beni Bousera peridotite massif, North Morocco: derivation from subducted oceanic lithosphere. Earth and Planetary Science Letters 102, 289–301.
Reagan, M.K., Ishizuka, O., Stern, R.J., Kelley, K.A., Ohara, Y., Blichert-Toft, J., Bloomer, S.H., Cash, J., Fryer, P., Hanan, B.B., Hickey-Vargas, R., Ishii, T., Kimura, J.-I., Peate, D.W., Rowe, M.C., Woods, M., 2010. Fore-arc basalts and subduction initiation in the Izu–Bonin–Mariana system. Geochemistry, Geophysics, Geosystems 11 Q03X12.
Rudnick,, 1995. Making continental crust. Nature 378, 571–578.
Saito, K., 1993. ^{40}Ar–^{39}Ar studies on some Tanzawa tonalite samples. Journal of Geomagnetism and Geoelectricity 45, 261–272.
Sato, K., Shibata, K., Uchiumi, S., 1986. Discordant K–Ar ages between hornblende and biotite from the Tanzawa tonalitic pluton in the southern Fossa Magna, central Japan. Journal of the Geological Society of Japan 6, 439–446.
Scholl, D.W., Vallier, T.L., Stevenson, A.J., 1987. Geologic evolution and petroleum geology of the Aleutian Ridge. In: Scholl, D.W., Grantz, A., Vedder, J.G. (Eds.), Geology and Resource Potential of the Continental Margin of Western North America and Adjacent Ocean Basins-Beaufort Sea to Baja California: Houston. Texas, Circum-Pacific Council for Energy and Mineral Resources, pp. 123–155.
Shillington, D.J., Van Avendonk, H.J., Holbrook, W.S., Kelemen, P.B., Hornbach, M.J., 2004. Composition and structure of the central Aleutian island arc from arc-parallel wide-angle seismic data. Geochemistry, Geophysics, Geosystems 5, Q10006. http://dx.doi.org/10.1029/2004GC000715.
Shimazu, M., 1989. Cenozoic volcanic activity in the South Fossa Magma. Modern Geology 14, 113–125.
Smith, T.E., Thirlwall, M.F., Macpherson, C., 1996. Trace element and isotope geochemistry of the volcanic rocks at Bequia, Grenadine islands, Lesser Antilles arc: a study of subduction enrichment and intra-crustal contamination. Journal of Petrology 37, 117–143.
Streckeisen, A., 1976. To each plutonic rock its proper name. Earth-Science Reviews 12, 1–33.
Sugiyama, A., 1976. Geologic development of the Tanzawa mountains, central Japan (Part I): stratigraphy and structure. The Journal of the Geological Society of Japan 82, 699–712.
Suyehiro, K., Takahashi, N., Ariie, Y., Yokoi, Y., Hino, R., Shinohara, M., Kanazawa, T., Hirata, N., Tokuyama, H., Taira, A., 1996. Continental crust, crustal underplating, and low-q upper mantle beneath an oceanic island arc. Science 272, 390–392.
Suzuki, K., Yamamoto, S., Sawaki, Y., Aoki, K., Omori, S., Kon, Y., Hirata, T., Li, Y., Takaya, Y., Fujinaga, K., Kato, Y., Maruyama, S., 2014. Zircon U–Pb dating from the mafic enclaves in the Tanzawa Tonalitic Pluton, Japan: implications for arc history and formation age of the lower-crust. Lithos 196–197, 301–320.
Takahashi, M., 1985. A proposal and development of granitoid series concept. The Memoirs of the Geological Society of Japan. 25 pp. 225–244.
Takahashi, M., 1989. Neogene granitic magmatism in the South Fossa Magna collision zone, central Japan. Modern Geology 14, 127–143.
Takahashi, M., Kanamaru, T., Nihira, S., 2004. Whole-rock chemistry of Tanzawa tonalite: summary of 171 samples. 39. Proceedings of the Institute of Natural Sciences Nihon University, pp. 259–284.
Takahashi, N., Kodaira, S., Klemperer, S.L., Tatsumi, Y., Kaneda, Y., Suyehiro, K., 2007. Crustal structure and evolution of the Mariana intra-oceanic island arc. Geology 35, 203–206. http://dx.doi.org/10.1130/G23212A.
Takita, R., 1974. Petrography and the plutonic history of the Tanzawa tonalite complex. Journal of the Geological Society of Japan 80, 505–523.
Tani, K., Dunkley, D.J., Kimura, J.-I., Wysoczanski, R.J., Yamada, K., Tatsumi, Y., 2010. Syncollisional rapid granitic magma formation in an arc-arc collision zone: evidence from the Tanzawa plutonic complex, Japan. Geology 38, 215–218.
Tatsumi, Y., Shukuno, H., Tani, K., Takahashi, N., Kodaira, S., Kogiso, T., 2008. Structure and growth of the Izu–Bonin–Mariana arc crust: 2. Role of crust–mantle transformation and the transparent Moho in arc crust evolution. Journal of Geophysical Research 113, B02203. http://dx.doi.org/10.1029/2007JB005121.
Taylor, H.P., Sheppard, S.M.F., 1986. Igneous rocks: I. Processes of isotopic fractionation and isotope systematics. In: Valley, J.W., Taylor Jr., H.P., O'Neil, J.R. (Eds.), Stable Isotopes in High Temperature Geological Processes. Reviews in Mineralogy 16. Mineralogical Society of America, Washington, D.C, pp. 227–271.
Taylor, S.R., White, A.J.R., 1965. Geochemistry of Andesites and the growth of Continents. Nature 208, 271–273.
Thirlwall, M.F., Graham, A.M., Arculus, R.J., Harmon, R.S., Macpherson, C.G., 1996. Resolution of the effects of crustal assimilation, sediment subduction, and fruid transport in island arc magmas: Pb–Sr–Nd–O isotope geochemistry of Grenada, Lesser Antilles. Geochemica et Cosmochimica Acta 60, 4785–4810.
Toriumi, M., Arai, S., 1986. Collision of Izu–Mariana arc from the point of view of metamorphism. Chikyu Monthly. 8 pp. 612–615.
Tunheng, A., Hirata, T., 2004. Development of signal smoothing device for laser ablation-ICP-mass spectrometer. Journal of Analytical Atomic Spectrometry 19, 932–934.
Valley, J.W., 2003. Oxygen isotopes in zircon. In: Hanchar, J.M., Hoskin, P.W.O. (Eds.), Zircon. Reviews in Mineralogy and Geochemistry. 53. Mineralogical Society of America, Washington, D.C, pp. 343–385.
Valley, J.W., Chiarenzelli, J.R., McLelland, J.M., 1994. Oxygen isotope geochemistry of zircon. Earth and Planetary Science Letters 126, 187–206.
Valley, J.W., Kinny, P.D., Schulze, D.J., Spicuzza, M.J., 1998. Zircon megacrysts from kimberlite: oxygen isotope variability among mantle melts. Contribution to Mineralogy and Petrology 133, 1–11.
Wang, Z., Eiler, J.M., 2008. Insights into the origin of low-$\delta^{18}O$ basaltic magmas in Hawaii revealed from in situ measurements of oxygen isotope compositions of olivines. Earth and Planetary Science Letters 269, 377–387.
Watson, E.B., Wark, D.A., Thomas, J.B., 2006. Crystallization thermometers for zircon and rutile. Contributions to Mineralogy and Petrology 151, 413–433. http://dx.doi.org/10.1007/s00410-006-0068-5.
Wiedenbeck, M., Hanchar, J.M., Peck, W.H., Sylvester, P., Valley, J., Whitehouse, M., Kronz, A., Morishita, Y., Nasdala, L., Fiebig, J., Franchi, I., Girard, J.-P., Greenwood, R.C., Hinton, R., Kita, N., Mason, P.R.D., Norman, M., Ogasawara, M., Piccoli, P.M., Rhede, D., Satoh, H., Schulz-Dobrick, B., Skår, O., Spicuzza, M.J., Terada, K., Tindle, A., Togashi, S., Vennemann, T., Xie, Q., Zheng, Y.-F., 2004. Further characterization of the 91500 zircon crystal. Geostandards and Geoanalysis 28, 9–39.
Yamada, K., Tagami, T., 2008. Postcollisional exhumation history of the Tanzawa tonalite complex, inferred from (U–Th)/He thermochronology and fission track analysis. Journal of Geophysical Research 113, B03402.
Yamamoto, Y., Kawakami, S., 2005. Rapid tectonics of the Late Miocene Boso accretionary prism related to the Izu–Bonin arc collision. Island Arc 14, 178–198.